

# Effect of $\text{TiO}_2$ on the interaction of dehydroxylated kaolinite with $\text{Al}(\text{OH})_3$ gel in relation to mullitisation

N.K. Mitra\*, A. Mandal, S. Maitra, A. Basumajumdar

*Department of Chemical Technology, University of Calcutta, 92, A P C Road, Kolkata 700 009, India*

Received 20 June 2001; received in revised form 3 July 2001; accepted 27 September 2001

## Abstract

Mullite being a material of prime importance in ceramics has drawn attention for a long time. Precursor powder for mullite was prepared in the active state by the aqueous phase interaction of dehydroxylated kaolinite and deposited aluminium hydroxide gel from  $\text{Al}(\text{NO}_3)_3$  solution. Magnitude of sintering as well as the sintered properties of the compacted mass was found to be influenced by the doping agent,  $\text{TiO}_2$ . © 2002 Published by Elsevier Science Ltd and Techna S.r.l.

**Keywords:** D. Mullite, D.  $\text{TiO}_2$ ; Dehydroxylated kaolinite

## 1. Introduction

Mixes of clay minerals, bauxite,  $\text{Al}(\text{OH})_3$  or alumina are used for the synthesis of commercial sintered mullite. The most commonly used clay mineral is kaolinite as it contains a relatively higher proportion of  $\text{Al}_2\text{O}_3$  and lower proportions of impurities. This type of mullite is designated as “Old mullite” in comparison to the term “New mullite” which represents high purity mullite (chemical mullite)[1]. The removal of the hydroxyl group from kaolinite during heating is accompanied by a reorganization of the octahedral layer of kaolinite to a tetrahedral configuration in metakaolin [2]. Different mechanisms [3–5] were proposed to take into account the nature of decomposition of metakaolin. Metakaolin decomposes, upon heating to an aluminium-silicon spinel and additional silica. A high degree of silicon incorporation into  $\gamma$ -alumina was also proposed [6], corresponding to 2/1 mullite composition while it was also suggested [7–9] that the  $\gamma$ -spinel was virtually pure  $\text{Al}_2\text{O}_3$ . Some workers [10,11] determined silicon incorporations up to 18 mol% silica and discussed temperature-dependant silicon incorporation mechanisms.

More recently researchers [12] determined the lattice parameters of mullite formed from kaolinite at greater than 1000 °C and found that these mullites are richer in

$\text{Al}_2\text{O}_3$  than stoichiometric mullite. Sintered mullite produced from clay minerals contains a considerable amount of impurities [13]. Some workers [14] tried to overcome these by using high purity kaolin and also by prolonged grinding of the starting material. Mechanochemical effects caused by prolonged grinding promote mullitisation [15] and, therefore, may also contribute to the enhancement of strength.

In the present work role of  $\text{TiO}_2$  as an additive on the sintering of dehydroxylated kaolinite and  $\text{Al}(\text{OH})_3$  gel mix for the formation of alumina-mullite composite was studied.

## 2. Experimental

English china clay was used in the present investigation. The clay was chemically analysed to ascertain its composition following conventional procedures and the result is giving in Table 1.

The clay was dehydroxylated at a temperature of 650 °C in an electrically heated muffle furnace and the heat treated clay was dispersed in requisite volume of  $\text{Al}(\text{NO}_3)_3$  solution. 1:2 ammonia solution was added slowly with thorough stirring so that no settling of the dehydroxylated clay powder occurred during gelation. Gelation took place at a pH of 8.5. The mixed gel was allowed to age for 24 h. The gel was properly washed to make it free from soluble electrolytes. The washed gel

\* Corresponding author. Fax: +91-33-361-9755.

E-mail address: chemtech@cucc.ernet.in (N.K. Mitra).

Table 1  
Chemical analysis of English china clay

| Constituents                   | Percent present in |                     |
|--------------------------------|--------------------|---------------------|
|                                | Raw clay           | Dehydroxylated clay |
| SiO <sub>2</sub>               | 48.30              | 55.52               |
| Al <sub>2</sub> O <sub>3</sub> | 37.75              | 42.53               |
| Fe <sub>2</sub> O <sub>3</sub> | 0.55               | 0.63                |
| CaO                            | 0.10               | 0.12                |
| LOI                            | 18.05              | –                   |

Table 2  
Chemical analysis of the dried precursor powder

| Constituents                   | Percent present | Molar ratio<br>SiO <sub>2</sub> :Al <sub>2</sub> O <sub>3</sub> |
|--------------------------------|-----------------|---|
|                                |                 |   |
| SiO <sub>2</sub>               | 26.01           | 1:1.61  |
| Al <sub>2</sub> O <sub>3</sub> | 71.20           |   |

was dried slowly at 55 °C and then ground and milled. Chemical analysis of the dried gel was carried out to ascertain the molar ratio of SiO<sub>2</sub> and Al<sub>2</sub>O<sub>3</sub> (Table 2).

DTA analysis of the gel was carried out in a NETZSCH simultaneous thermal analyzer (STA-409) with a heating rate of 10 °C/min. Infrared analysis of the gel sample was carried out in infrared spectro-

Table 3  
Composition of the batches

| Batch No. | TiO <sub>2</sub> (wt.%) |
|-----------|-------------------------|
| I         | 0                       |
| II        | 1.0                     |
| III       | 1.5                     |
| IV        | 2.0                     |

photometer of Perkin Elmer (model 287). TiO<sub>2</sub> in different percentages was mixed with the dried hydrogel (Table 3). The mixing was carried out in acetone medium with thorough shaking followed by evaporation of the solvent.

The samples were compacted at a pressure of 120 MPa and sintered in an electrically heated muffle furnace at temperatures of 1400, 1500, 1550 and 1600 °C with 2 h soaking period. Firing shrinkage, apparent porosity, bulk density and true density of the sintered compacts were measured following conventional procedures. Thermal spalling resistance of the samples was carried out by the water quenching method. Flexural strength of the sintered composites was measured by the 3-point bending method at a temperature of 800 °C. X-ray analysis of the samples was carried out with X-ray diffractometer (Philips PW1730) using CuK<sub>α</sub> radiation. SEM analysis of the samples was carried out in Leo Electron Microscope, Cambridge.

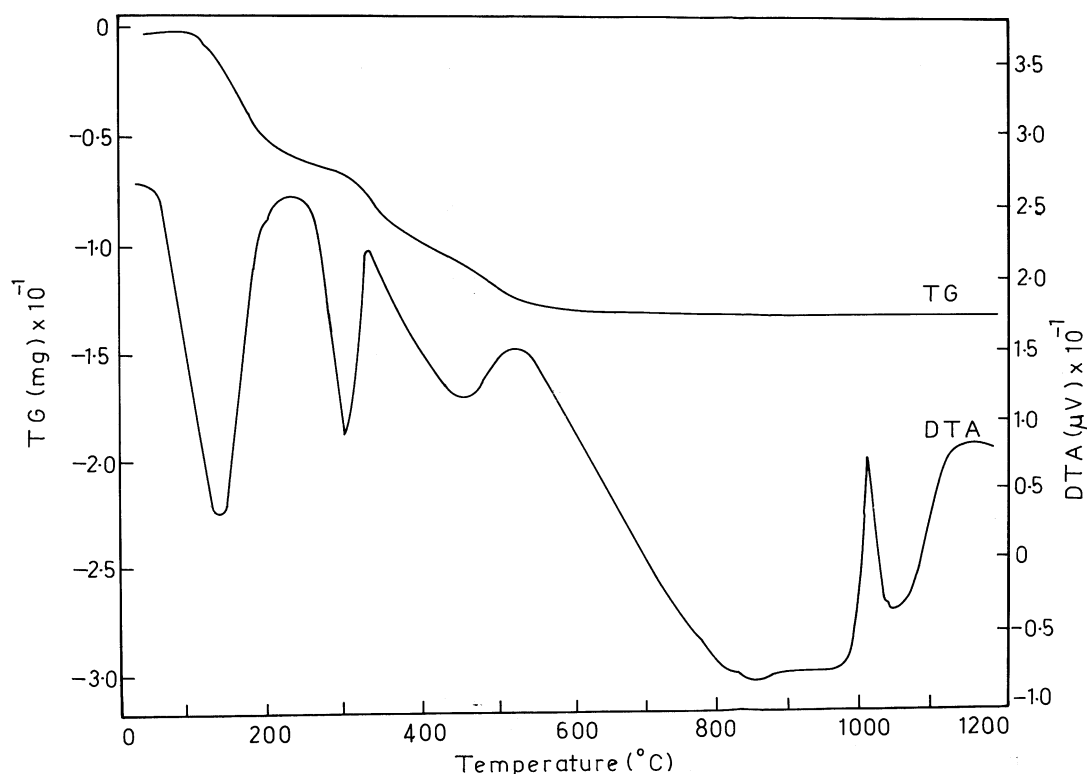


Fig. 1. Differential thermal analysis and thermo-gravimetric analysis of alumina-silica precursor powder (doped with 1.5 wt.% TiO<sub>2</sub>).

### 3. Discussion

Dehydroxylated clay contained about 42.5%  $\text{Al}_2\text{O}_3$ . The molar ratio of  $\text{SiO}_2:\text{Al}_2\text{O}_3$  in the precursor powder was kept at 1:1.61 i.e., which was above the traditional mullite zone. The texture of the precursor powder

was very fine and the surface area was found to be  $120 \text{ m}^2/\text{gram}$ , which was sufficient enough for better compaction.

The initial endothermic peak at  $150^\circ\text{C}$  in the DTA diagram (Fig. 1) was associated with the expulsion of loosely bound gel water. The second endothermic peak

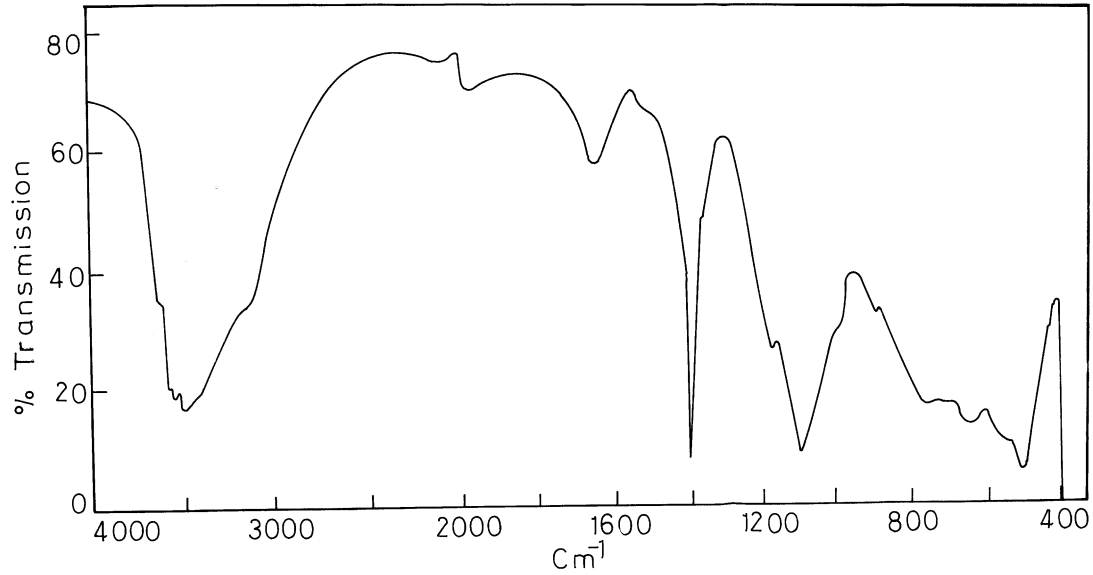


Fig. 2. Infrared analysis of alumina-silica precursor powder (doped with 1.5 wt.%  $\text{TiO}_2$ ).

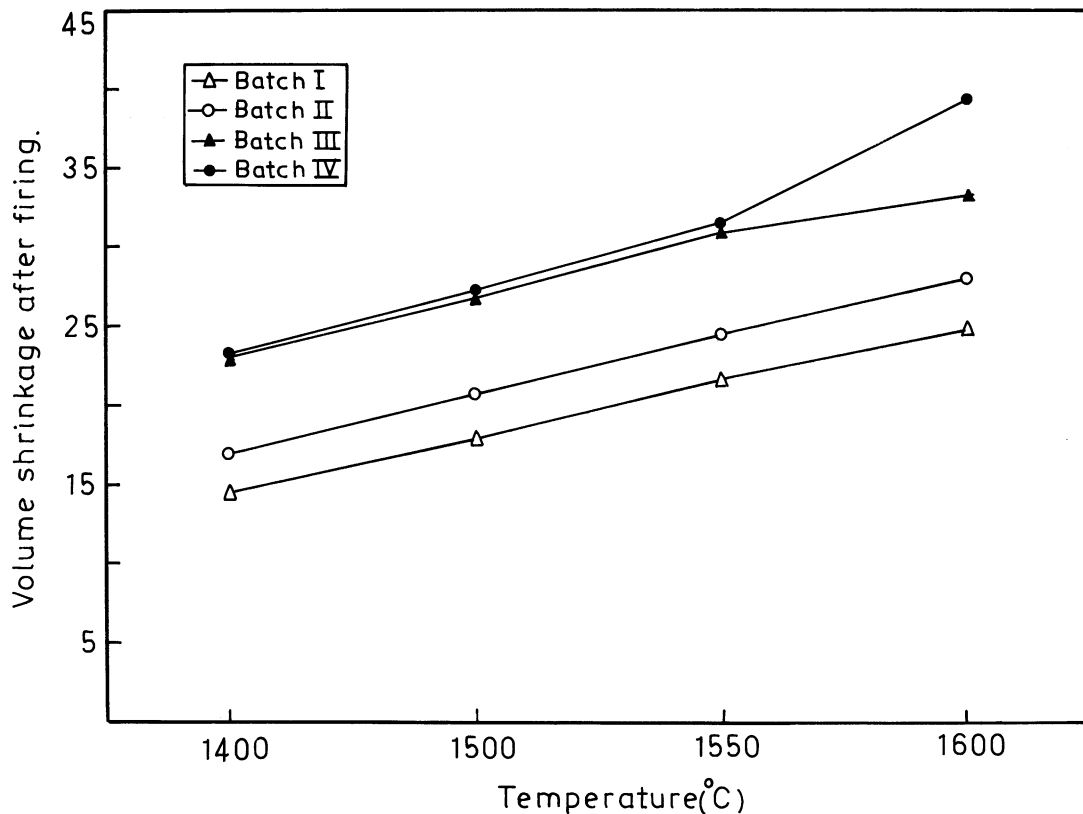


Fig. 3. Volume shrinkage vs temperature curves of samples fired at different temperatures.

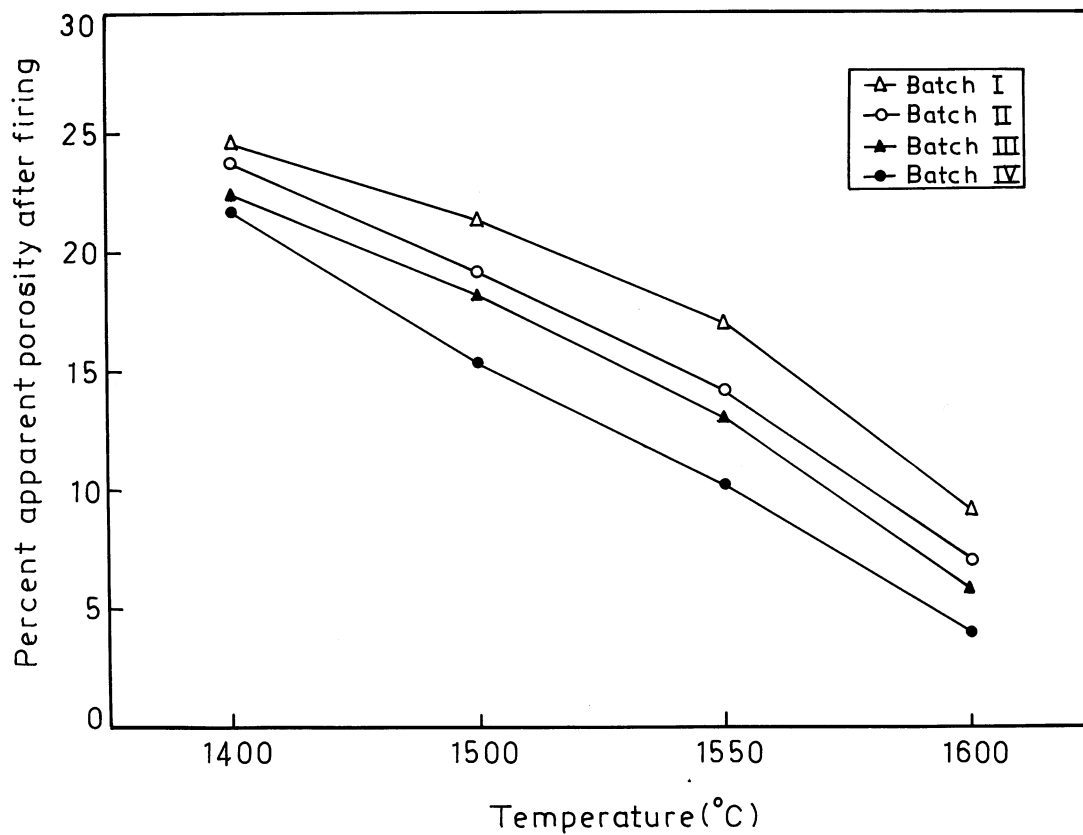


Fig. 4. Apparent porosity vs temperature curves of samples fired at different temperatures.

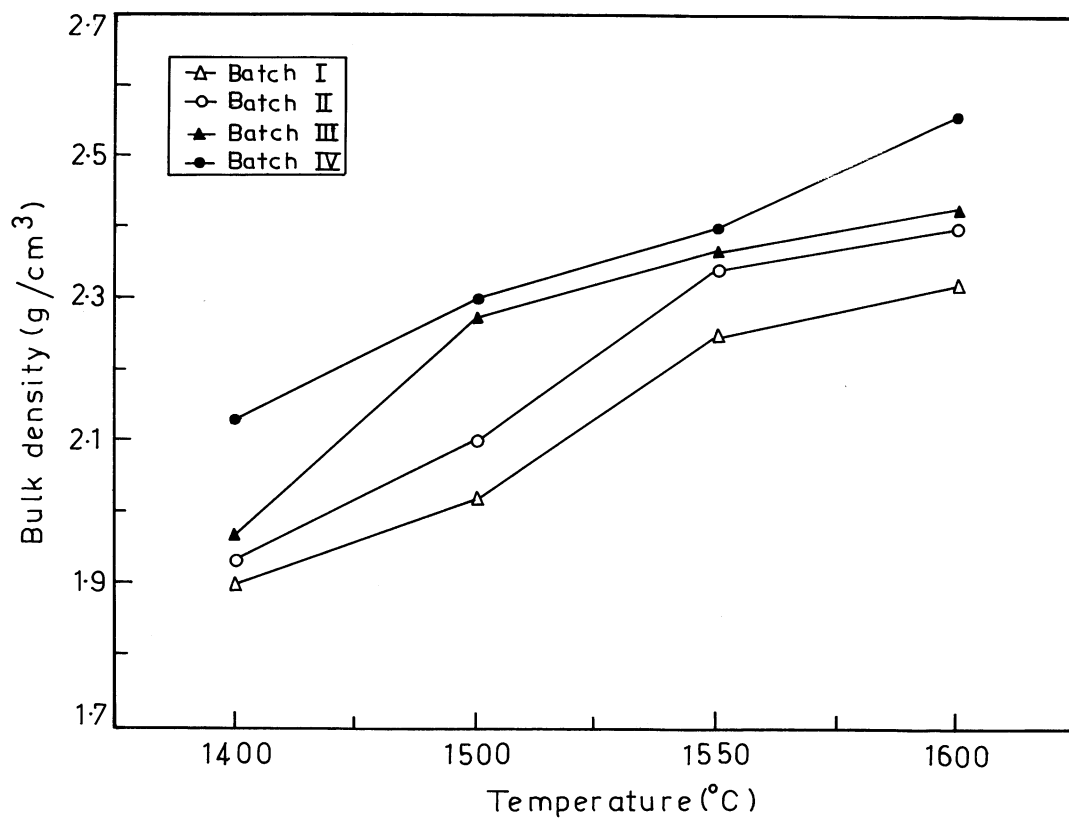


Fig. 5. Bulk density vs temperature curves of samples fired at different temperatures.

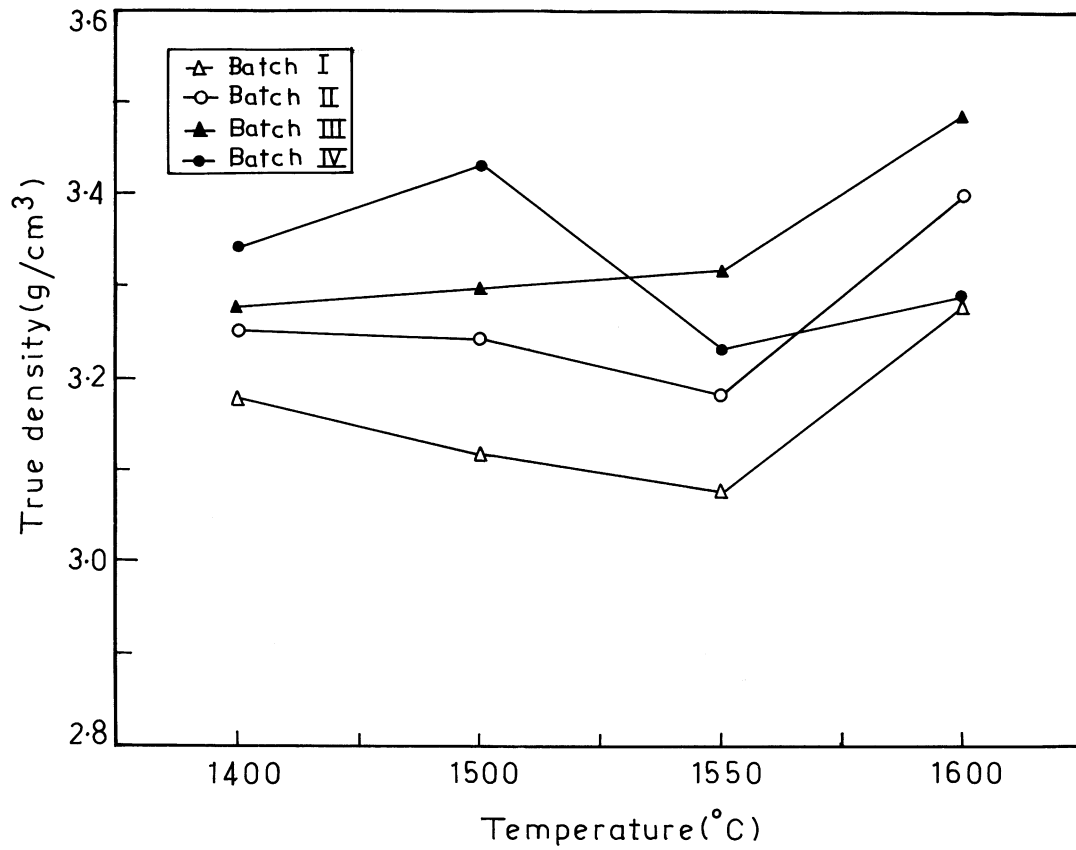


Fig. 6. True density vs temperature curves of samples fired at different temperatures.

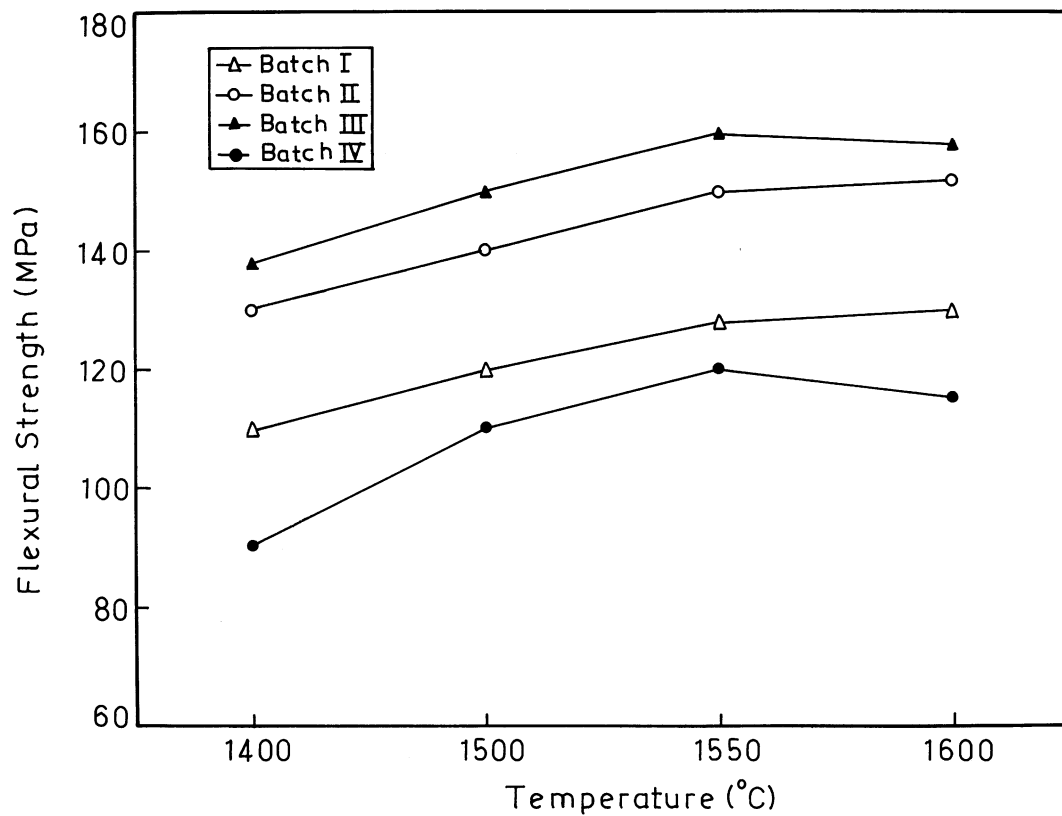


Fig. 7. Flexural strength vs temperature curves of samples fired at different temperatures.

at 300 °C represented the formation of  $\gamma$ -Al-O-OH from  $\text{Al}(\text{OH})_3$ . The sharp exothermic peak at 1030 °C might be due to formation of an Al/Si spinel prior to mullitisation.

In the IR spectra of the gel material (Fig. 2) the strong absorption peak at about  $3500\text{ cm}^{-1}$  was related to the -OH stretching vibration. This was contributed mainly by aluminium hydroxide gel as dehydroxylated kaolinite does not exhibit such vibration due to complete breakage of metal-hydroxyl bond. The frequency band at  $1080\text{ cm}^{-1}$  is related to the perpendicular vibration of Si-O bond. The Al-O stretching vibration was also observed in the spectrum. The absorption band at  $1630$

and  $1400\text{ cm}^{-1}$  was ascribed to O-H bending vibrations. So the physical identity of both  $\text{Al}(\text{OH})_3$  and dehydroxylated kaolinite was retained in the gel sample.

Appreciable volume shrinkage of the samples was observed after sintering (Fig. 3) and it increased with the increase in sintering temperature as well as the mineraliser content. At high temperature liquid formation is expected in the alumina-silica system, which causes appreciable shrinkage. The mineraliser i.e.  $\text{TiO}_2$  influenced the shrinkage probably via the formation of more liquid phases like aluminium titanate. The sharp increase of shrinkage at 1600 °C may be related to the formation of more liquid phase. The nature of the

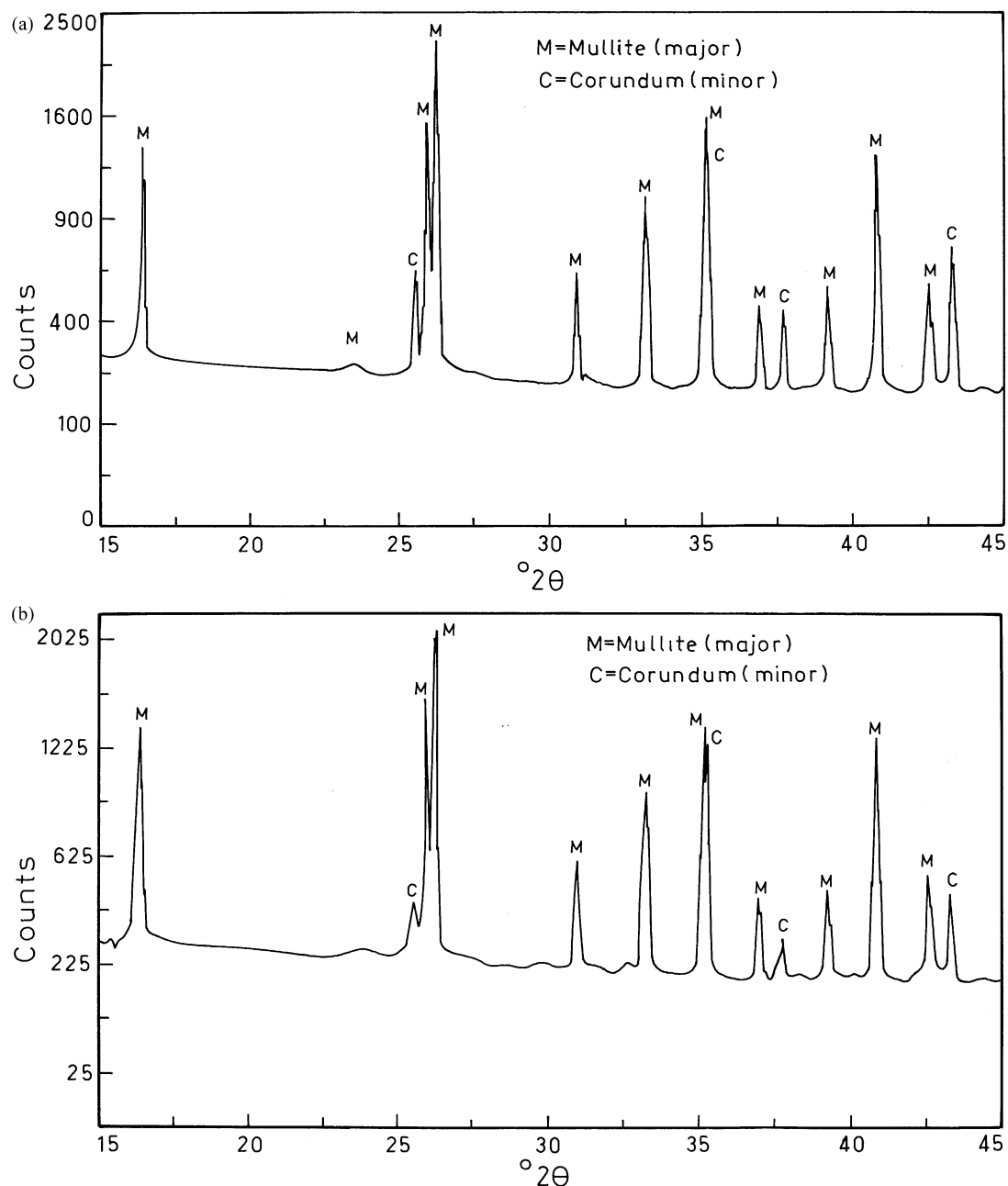


Fig. 8. XRD diagram of samples sintered at 1500 °C. (a) batch I; (b) batch II; (c) batch III; (d) batch IV.

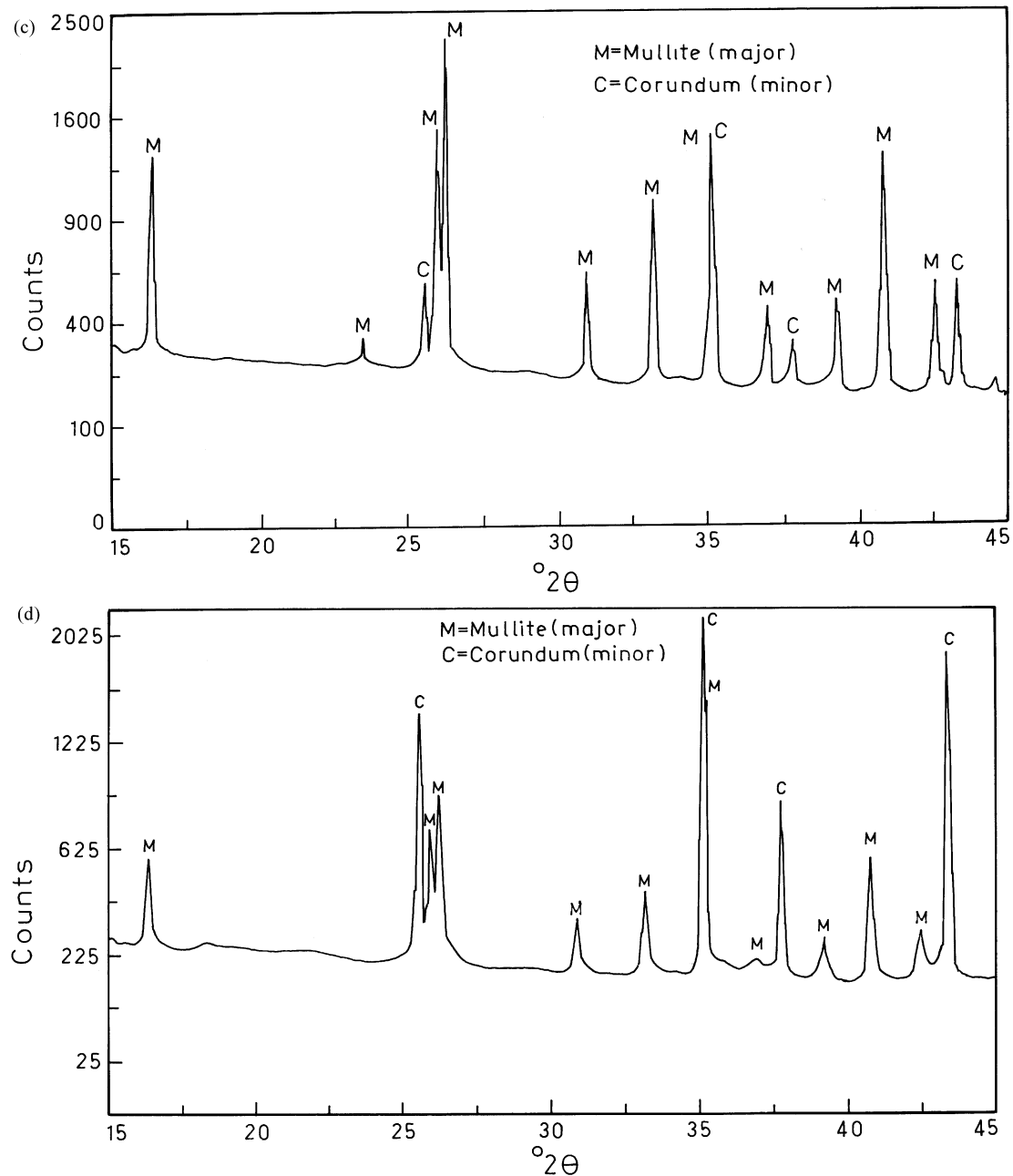


Fig. 8. (continued)

curves did not exhibit any significant variation with change in  $\text{TiO}_2$  content except batch No. IV with the maximum amount of mineraliser, which showed an inflexion at  $1550^\circ\text{C}$ . Probably formation of additional liquid phases is responsible for this.

Apparent porosity values in the sintered compacts (Fig. 4) were found to decrease with the increase in sintering temperature. Porosity values were also found to decrease with the increase in the  $\text{TiO}_2$  content in the composition indicating the formation of more liquid phases in the batches. Sufficient porosity was retained in the sintered products, which might be due to the

presence of more alumina in excess of conventional mullite.

From bulk density values of the sintered samples (Fig. 5), it was observed that 70–80% densification was achieved at  $1600^\circ\text{C}$ . At  $1400^\circ\text{C}$ , bulk density was very low which was indicative of low sinterability. The nature of the curves was not similar which clearly indicates the role of  $\text{TiO}_2$  on the sintering behaviour.

From an analysis of the true density values (Fig. 6) it was evident that there was positive formation of mullite-alumina in the sintered products. At the highest temperature of firing the density values were inversely

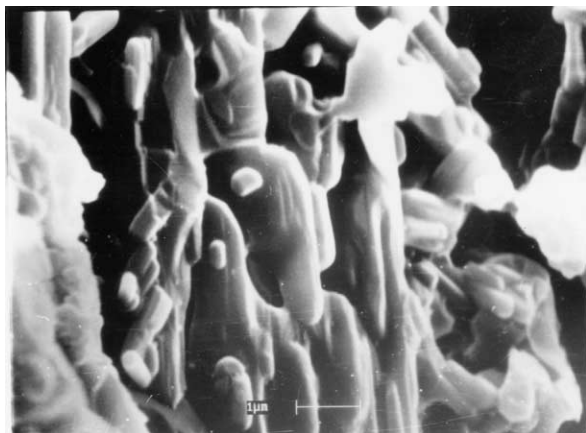


Fig. 9. SEM photomicrograph of sintered compacts of batch II.

related to  $\text{TiO}_2$  content in the batches. A steep increase in density at 1600 °C may be due to separation of more corundum phases by peritectic transformation. In case of batches II and IV, reduction of density at 1500 °C may be due to the formation of more liquid phases in the sintered compacts.

All these sintered pellets were subjected to thermal spalling in an accelerated process i.e. heating at 800 °C for 10 min and then quenching under water for 10 min. The operation was carried out up to 8 cycles and the general observation was that no visible crack formation occurred in any one of the sample. The spalling resistance generated in the samples may be due to the formation of less glassy phase and generation of low expansion aluminium titanate phase at the grain boundaries.

Flexural strengths of the sintered compacts (Fig. 7) increased with the increase in sintering temperature as well as the mineraliser content. This clearly indicated positive role of  $\text{TiO}_2$  on the sinterability of the composites.

From the XRD diagrams of the samples (Fig. 8a–d) mullite was found to be the major crystalline phase

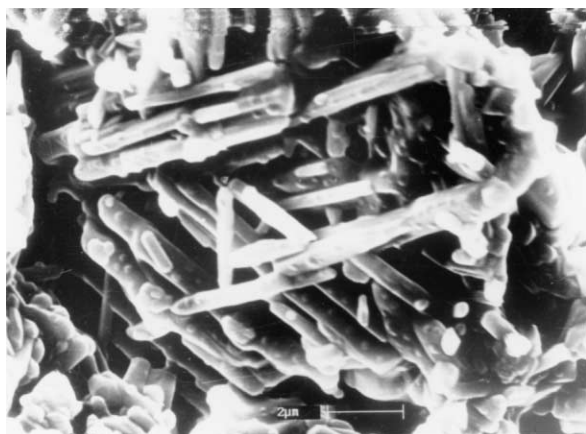


Fig. 10. SEM photomicrograph of sintered compacts of batch III.



Fig. 11. SEM photomicrograph of sintered compacts of batch IV.

followed by corundum ( $\alpha\text{-Al}_2\text{O}_3$ ) in all the compositions. The content of mullite followed an inverse relationship with the dopant concentration. No  $\text{TiO}_2$  bearing major crystalline phases was observed in the sintered compacts.

SEM micrographs of the sintered samples with additive are shown in Figs. 9–11. In all the micrographs, needle like mullite crystals were observed to be the major phase. With the increase in  $\text{TiO}_2$  content, amount of glassy phase in the intergranular position, increased. Uniform distribution of interlocked mullite crystals in the sintered masses suggested the development of appreciable physico-mechanical properties in these composites. Tetragonal corundum phases were also observed in the micrographs. Increase in the  $\text{TiO}_2$  content was found to reduce intergranular porosity in the materials.

#### 4. Conclusion

$\text{TiO}_2$  plays a positive role in the formation of mullite by reactions between dehydroxylated kaolinite and incipiently formed  $\text{Al}(\text{OH})_3$  gel through wet interaction. With the increase in  $\text{TiO}_2$  content, porosity of the sintered compacts decreased and bulk density increased.  $\text{TiO}_2$  probably formed titania bearing liquid phase under the experimental condition (up to 1600 °C) which promoted sintering and therefore no titania bearing crystalline phases was observed in the XRD diagram of the sintered compacts, although the batches contained higher proportion of alumina compared to conventional mullite composition.

#### References

- [1] H. Schneider, K. Okada, J. Pask, *Mullite and Mullite Ceramics*, John Wiley & Sons, 1995, pp. 115–116.
- [2] S. Iwai, H. Tagai, T. Shimamune, Procedure for dielectric structure



- modification by dehydration, *Acta Crystallogr. B* 27 (1971) 248–250.
- [3] A.K. Chakrabarty, D.K. Ghosh, Comment on Interpretation of the kaolinite-mullite reaction sequence from infrared absorption spectra, *J. Am. Ceram. Soc.* 61 (1978) 90–91.
- [4] A.K. Chakrabarty, D.K. Ghosh, Re-examination of kaolinite to mullite reaction series, *J. Am. Ceram. Soc.* 61 (1978) 170–173.
- [5] K. Srikrishna, G. Thomas, R. Martinez, M.P. Corral, S. De Aza, J.S. Moya, Kaolinite-mullite reaction series; a TEM study, *J. Mater. Sci.* 25 (1990) 607–612.
- [6] I.M. Low, R. McPherson, The origins of mullite formation, *J. Mater. Sci.* 24 (1989) 926–936.
- [7] W. Ch Wei, J.W. Halloran, Phase transformations of diphasic aluminosilicate gels, *J. Am. Ceram. Soc.* 71 (1988) 166–172.
- [8] M.J. Hyatt, N.P. Bansal, Phase transformations in xerogels of mullite compositions, *J. Mater. Sci.* 25 (1990) 2815–2821.
- [9] J.S. Lee, S.C. Wu, A characterization of mullite prepared from coprecipitated  $3\text{Al}_2\text{O}_3 \cdot 2\text{SiO}_2$  powder, *J. Mater. Sci.* 27 (1992) 5203–5208.
- [10] K. Okada, N. Otsuka, Change in chemical composition of mullite formed from  $2\text{SiO}_2 \cdot 3\text{Al}_2\text{O}_3$  xerogels during the formation process, *J. Am. Ceram. Soc.* 70 (1987) C245–C247.
- [11] H. Schneider, D. Voll, B. Saruhan, L. Merhin, A. Sebald, Mullite precursor phases, *J. Eur. Ceram. Soc.* 11 (1993) 87–94.
- [12] K. Okada, N. Otsuka, Chemical composition of change of mullite during formation process, *Sci. Ceram.* 14 (1988) 497–502.
- [13] K. Okada, N. Otsuka, S. Somiya, Review of mullite synthesis roots in Japan, *Am. Ceram. Soc. Bull.* 70 (1991) 1633–1640.
- [14] K. Hamano, S. Okada, H. Nakajima, F. Okuda, Preparation of mullite ceramics from kaolin and aluminium hydroxide, Abstracts of the Annual Meeting of the Ceramic Society of Japan, Paper No. F 205, Ceramic Society of Japan, Tokyo, 1991.
- [15] S. Kawai, M. Yoshida, G. Hashizume, Preparation of mullite from kaolin by dry-grinding, *J. Ceram. Soc. Jpn.* 98 (1990) 669–674.